# Indirect aircraft structural monitoring using artificial neural networks

**S. C. Reed**
QinetiQ
Farnborough, UK

## ABSTRACT

From necessity, military aircraft often operate in a highly fatigue damaging environment and history has shown in lost lives and aircraft the consequences of failure to appreciate fully the usage environment. The need for robust and cost effective structural usage monitoring of military aircraft to ensure operations are conducted within acceptable levels of risk is paramount. Furthermore, increased economic pressures require ever-inventive methods to be employed to maximise the lives of military fleets; structural usage monitoring will be a key asset in this drive. A highly cost effective indirect structural health and usage neural network (SHAUNN) monitoring system is proposed. A SHAUNN uses regression relationships determined by artificial neural networks to predict stresses, strains, loads, or fatigue damage from flight parameters. Within this paper the development of a SHAUNN monitoring system is described. Flight parametric data, captured during Operational Loads Measurement of the Royal Air Force Dominie TMk1 aircraft have been used to predict stresses at the key structural location in the wing, using mapping relationships determined by artificial neural networks. A framework for the development of the SHAUNN monitoring system is discussed and the basic architecture of the multilayer perceptron artificial neural network is described. It is concluded that this technology could provide the basis for an accurate, cost-effective structural usage monitoring system and further work to investigate the prediction of ground –based stresses in the wing is recommended.

## NOMENCLATURE

| | |
|---|---|
| ALT | altitude |
| ANN | artificial neural network |
| ARINC | Aeronautical Radio Incorporated |
| ASTM | American Society for Testing and Materials |
| BANK | inclinometer angle |
| DAU | data acquisition unit |
| DYP | dynamic pressure |
| EAS | equivalent airspeed |
| FFT | fast fourier transform |
| FI | fatigue index |
| ft | feet (altitude) |
| g | acceleration due to gravity ($9{\cdot}81 ms^{-1}$) |
| GAG | ground-air-ground cycle |
| IAT | individual aircraft tracking |
| IVS | independent validation set (data) |
| Logsig | logistic sigmoid activation function |
| MOD | Ministry of Defence (UK) |
| MLP | multi layer perceptron |
| MSE | mean squared error |
| NY | lateral acceleration |
| NZ | normal acceleration |
| NZW | normal acceleration conditioned by mass |
| OAT | outside air temperature |
| OLM | operational loads measurement (fixed wing) |
| PCA | principal components analysis |
| PSD | power spectral density |

**Paper No. 3152**. Manuscript received 3 November 2006, revised 31 March 2008 accepted 9 April 2008.

https://doi.org/10.1017/S0001924000002190 Published online by Cambridge University Press

| | |
|---|---|
| PW4,5,6 | port wing 4,5,6 (dominie monitor locations) |
| R | correlation coefficient |
| RAF | Royal Air Force |
| RMS | root mean squared |
| samples/s | samples per second |
| SHAUNN | structural health and usage neural networks |
| SHM | structural health monitoring |
| S-N | stress – endurance curve |
| SPC | sortie profile codes |
| SW4,5,6 | starboard wing 4,5,6 (dominie monitor locations) |
| TMk1 | trainer mark 1 |
| W | mass |
| WOW | weight-on-wheels |

Note: Non-conventional nomenclature was used for many of the flight parameters to match variables declared within the SHAUNN software to prevent transcription errors between code and software documentation.

## 1.0 INTRODUCTION

Maximising an aircraft's reliability, availability, performance and safe fatigue life is paramount. Today, avionic and weapons systems and even engines can be replaced or upgraded and therefore, the safe fatigue life of the aircraft structure will increasingly be one of the key factors that define the economic life-limit of a military aircraft fleet. A fleet-wide direct strain-based system would offer a solution in principle for most structural usage monitoring requirements and such a system is being introduced with the UK Eurofighter-Typhoon fleet[1]. However, these systems are costly to develop and support. Furthermore, experience has also shown that strain gauge installations are often vulnerable to in-service damage. Although measures can be taken to protect gauge installations, these protective measures often impede repair of gauge installations when they do fail. Hence, alternative, more cost-effective solutions should be investigated.

Parametric-based usage monitoring systems could offer a cost-effective solution and the mechanism for using a parametric-based individual aircraft tracking (IAT) system is well established in the UK; the fatigue meter and associated fatigue meter formulae have been the backbone of UK military IAT systems for the past 40 or 50 years. Additionally, most of the inputs needed for a flight parameter based system are already available on a modern military aircraft, through data bus systems. Flight control, weapons management and fuel systems all use similar parametric data; hence, in principle, an indirect usage monitoring system, using parametric inputs to predict strains, stresses or loads, has the potential to offer a cost-effective solution. Also, an indirect system could still have a role to play for strain-based fleet-wide monitoring systems. Parametric predictions could be used to provide back-up facilities for failed strain sensors, pending repair and as a vehicle to provide continuous monitoring of strain outputs by comparing the predicted and recorded strains and highlighting unexpected deviations.

However, there are drawbacks and issues to address with indirect usage monitoring systems; determining the relationship between parameters and stresses, strains or loads can be extremely complex. Also, it is essential to have methods to identify when those relationships have changed. Artificial neural networks (ANN), used to map parameters to stresses, strains or loads, have the potential to address some of these issues; they have the characteristics of being able to learn from experience, generalise from examples and identify underlying information from noisy data. However, they would need to be developed within a framework where confidence could be assured in the prediction made by the ANN throughout the service life of the aircraft.

Most notable in the work of others in this field, Azzam *et al*[2,3] and Wallace *et al*[4] described the use of a 'mathematical network' to predict loads and described cooperative work programmes involving ESS Smiths, the UK Ministry of Defence and BAE Systems. Successes reported included excellent correlation between measured and predicted strains at a number of structural locations for the Tornado combat aircraft, over a large number of test flights. Azzam *et al*[3] also described the development of methods to predict damage in helicopter components and the prediction of high-frequency events, or rare events as he termed them, such as buffet loading on the fin of a fixed-wing aircraft.

In addition, Jacobs and Perez[5] used a hybrid cascade ANN to augment sparse buffet data by predicting the power spectral densities of surface pressures on a fighter aircraft vertical tail, from parametric data. Kim and Marciniak[6] reported the use of a back-propagation ANN to predict strains in the empennage of a Cessna 172P General Aviation aircraft during discrete manoeuvres. Hill *et al*[7] described the use of a back-propagation ANN to synthesise strain and fatigue damage in several Lynx helicopter components. Furthermore, Manry and co-authors[8] applied ANNs to flight load synthesis, using Bell helicopter data. Levinski[9] used ANN technology to synthesise loads on the vertical tail of a F/A-18 aircraft, using wind-tunnel pressure data. Wang[10] used a recurrent ANN to predict loads during discrete manoeuvres for a fighter aircraft.

The work reported here is a further development of that described in Reed and Cole[11] and Reed[12, 13] in which the development of an ANN-based parametric fatigue monitor for the wing and tailplane of a military trainer aircraft and the wing of a combat aircraft were described.

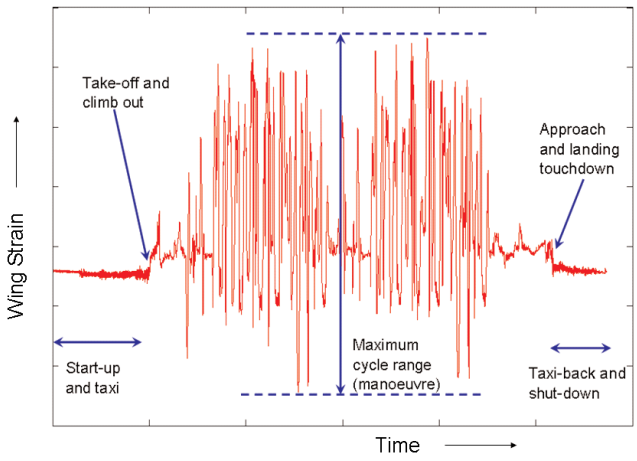



Figure 1. Example combat or trainer inner wing strain time history.

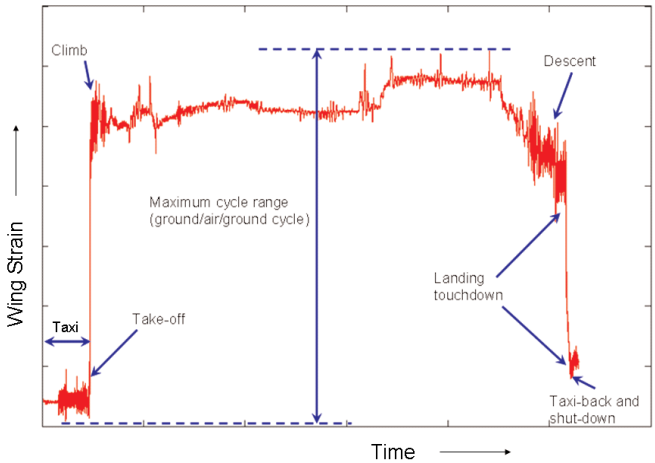



Figure 2. Example large aircraft inner wing strain time history.

https://doi.org/10.1017/S0001924000002190 Published online by Cambridge University Press

## 2.0 AIM

The wing strain prediction studies previously reported[11,12,13] were undertaken using data from relatively small, stiff aircraft. For these aircraft, the significant changes in strains in the wing monitoring locations were dominated by pilot-induced manoeuvre loading, with the addition of gust loads during low-level flying. These models achieved high overall strain correlations between prediction and target values and extremely accurate damage predictions for previously unseen data; however, the errors seen in the strain predictions often occurred when the aircraft was on the ground. For relatively stiff aircraft the implications of this, in fatigue damage terms, were often negligible, due to the dominance of the manoeuvre-induced strain cycles in the fatigue damage sum. This is illustrated in Fig. 1, where a typical wing strain time history for a combat aircraft or associated trainer is shown. Furthermore, the changes in mean stress or strain level seen in the wings during take-off and landing were relatively small for these aircraft, compared with the range of the cycles seen during the airborne phase of the sortie. Therefore, the fatigue damage accrued for the flight would be dominated by the large manoeuvre strain cycles incurred while airborne.

Conversely, for larger aircraft, such as transport, tanker or large trainer aircraft, the characteristics of the strain or stress time history for the wing are very different and this is illustrated in Fig. 2.

In the large-aircraft example, the fatigue damage accrued during the sortie would be dominated by the maximum cycle in the stress time history, the ground-air-ground (GAG) cycle, as it is termed. This cycle would generally be formed from a minimum value, or trough, when the aircraft was on the ground, to a maximum value, or peak, when the aircraft was airborne. The minimum stress value would usually occur at the beginning of the flight, often during the run-up against the brakes just before take-off, when the aircraft was heaviest and the wings were full of fuel. Hence, the wing lower skin would be in maximum compression. As the take-off run commenced, the wing lift would increase and the weight of the aircraft would increasingly be supported by the air load, primarily over the wings, and the loading on the wing lower surface would become tensile. The 'air' part of the GAG would be the peak tensile load seen in the wings during the airborne phase and this could be a result of gust load, manoeuvre load or purely aerodynamic loading. Occasionally, despite the aircraft being, generally, significantly lighter on landing than take-off, the maximum trough (maximum compressive load) could occur during the landing phase, due to the dynamics of the landing touchdown.

Therefore, the aim of the work outlined in this paper was to predict the stresses in the wing of a larger civil or civil-derivative aircraft used in a military environment. Data from the RAF Dominie TMk1 wing OLM programme was used to develop SHAUNN models to predict wing stresses from flight parameters. The Dominie TMk1 is a military derivative of the Hawker Siddeley HS125 and the aircraft is powered by two Bristol Siddeley Viper 520 turbojets. The aircraft has a length of 14·48m and a span of 14·33m and has a crew of two with three navigator training positions. The civil version of the aircraft is generally classed as a business jet.

A target correlation coefficient between predicted and 'measured' stress of 0·995 for unseen data was set for this study, based upon 'accuracy' levels specified for a recently developed parametric-based military aircraft structural monitoring system. Additionally, a target of +/-10% was set for an overall fatigue damage sum comparison between the predicted and measured stress time histories for the same data set, based upon historic targets for UK military monitoring systems.

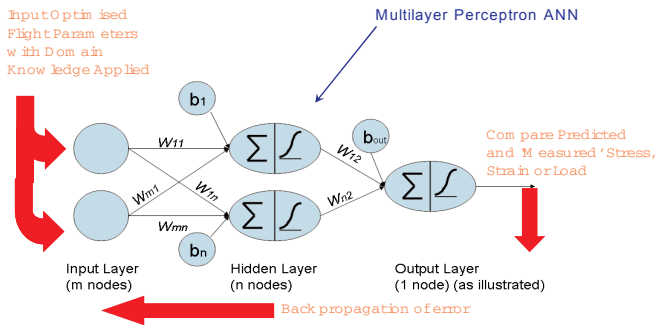



Figure 3. SHAUNN supervised learning.

## 3.0 SHAUNN ARCHITECTURE

Artificial neural networks (ANN) are attractive tools for use within indirect monitoring systems because of their ability to learn from experience, generalise from examples and identify underlying information from noisy data. The kernel of the SHAUNN was a single hidden-layer multilayer perceptron (MLP) ANN[14] with logistic sigmoid non-linear activation units. The network was trained in sequential mode, using a gradient descent algorithm with fixed learning rate and a momentum coefficient. The use of large training data sets (several hundred thousand lines) allowed relatively simple training methods to be used to form well-generalised solutions, with little risk of over fitting. The supervised learning techniques used in this application is illustrated schematically in Fig. 3.

## 4.0 MILITARY USAGE OF CIVIL-DERIVATIVE AIRCRAFT

For large aircraft, operating in a civil-type operating environment (as seen in Fig. 2), where the sortie can be simply described as take-off, climb to cruise altitude, cruise, descent, land and taxi-back, the fatigue damage seen in the wings will largely be dominated by the GAG cycle. Military operations, however, are not restricted to civil-type flights and military derivatives of civil aircraft are often used in roles significantly different to those for which they were designed. Usage monitoring in the military arena has, historically, been concentrated upon combat aircraft and associated trainers. However, combat aircraft were designed to be operated to combat aircraft usage.

Flight types for all UK military aircraft are divided into Sortie Profile Codes (SPC). These SPCs are used as a method of segregating flights into similar groups for trending and further analysis. Therefore, for a combat aircraft, for example, these SPCs might include air-to-air combat, ground attack, air display etc. The Dominie has 13 SPCs, which cover all the operations of the aircraft. However, rather than generating 13 different models, analysis of Dominie flight data identified that the sorties could be naturally divided into four groups. These groups were termed Type 1-4 and identified as 'civil transport', low-level', 'maritime' and 'training' and particular SPCs were mapped to each group.

Civil transport sorties were, as the name suggests, typical of civilian transport type flights, generally consisting of: taxi, take-off, climb to cruise altitude (e.g. 31,000ft), cruise, descent, landing and taxi back. The majority of the flight was conducted at medium-to-high altitudes, above the severe gust regime (>10,000ft), and rarely was more than one roller (or touch-and-go) landing undertaken. A typical altitude, airspeed, normal acceleration and wing stress profile for a civil transport flight is reproduced in Fig 4(a) (for comparison, corresponding plots for the remaining flight types are reproduced in Fig 4(b), 4(c) and 4(d), using the same scale). Civil transport type flights were generally benign and the fatigue damage was dominated by the GAG cycle.

https://doi.org/10.1017/S0001924000002190 Published online by Cambridge University Press

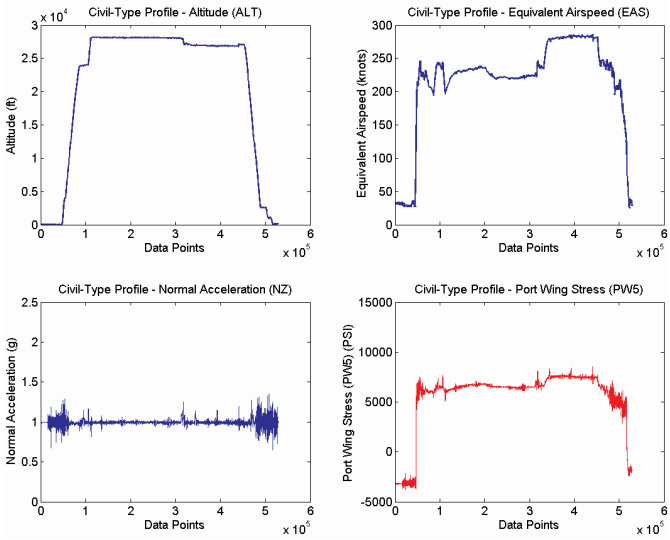



Figure 4(a). Example 'civil transport' flight profile.

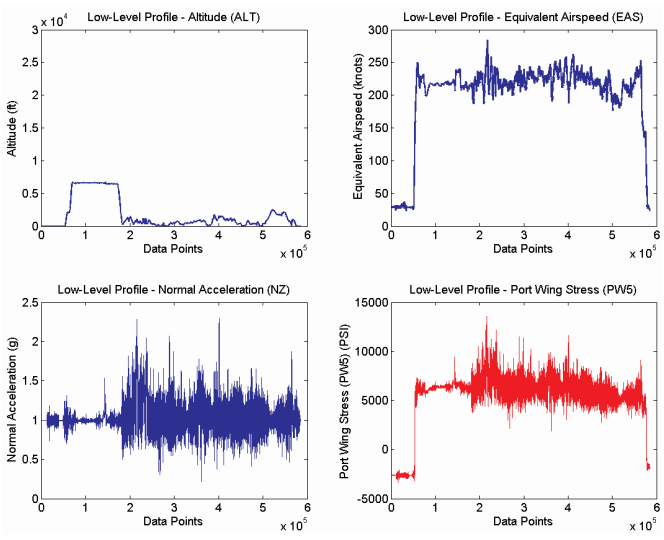



Figure 4(b). Example 'low-level' flight profile.

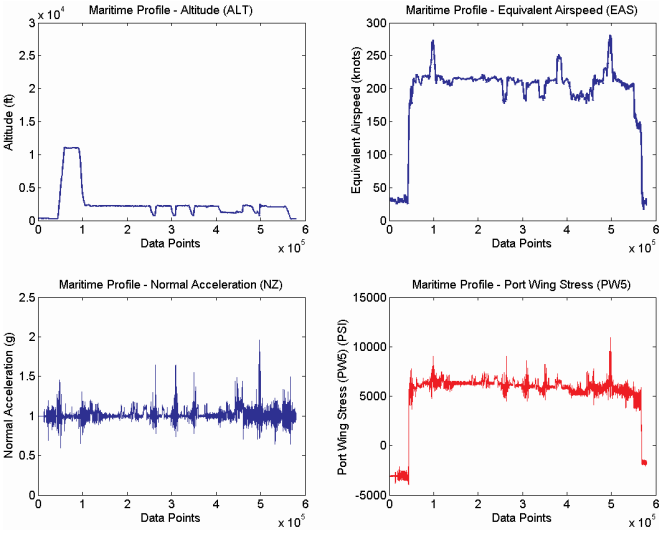



Figure 4(c). Example 'maritime' flight profile.

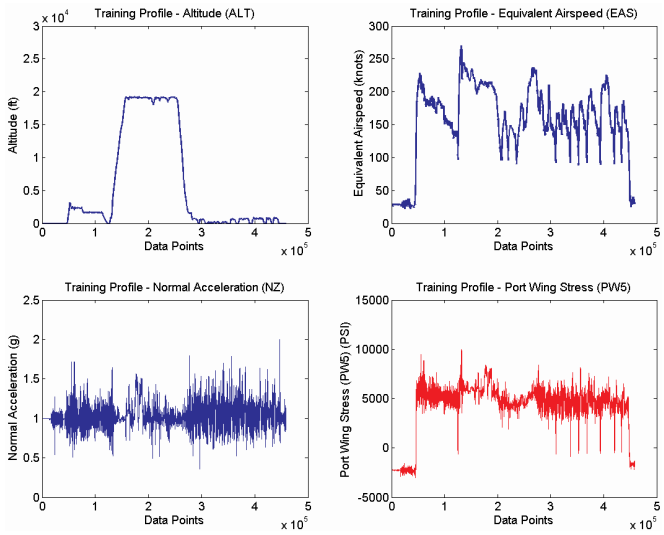



Figure 4(d). Example 'training' flight profile.

Even a cursory glance at Fig. 4(a) reveals that there is an obvious correlation between Equivalent Airspeed (EAS) and the mean stress in the wing, for this type of sortie. Gust loading was evident in the wing stress profile during the climb and descent phases of the flight and these regions were matched with responses in the normal acceleration (NZ) data. The character of these sorties was very different to combat aircraft wing data, where normal acceleration was by far the dominant parameter throughout the sortie.

Low-level sorties (Fig. 4(b)) however were found to have a very different character in their profiles. Here the majority of the sortie was flown at low-level over land (often 1,500ft or below). Hence, the aircraft was operating in a severe turbulence environment and the effect of gust loading for these sorties flown over the land was immediately evident on the stress and normal acceleration channels. For the low-level profile, the mean stress in the wing still followed the equivalent airspeed plot but the gust loading, which followed the normal acceleration plot, was superimposed upon it. The normal acceleration variation was primarily attributed to gust loading, due to its symmetry about 1·0g. Spectra that are manoeuvre-dominated (e.g. combat aircraft) have far greater content above 1·0g than below 1·0g.

Maritime sorties (Fig. 4(c)) often had very similar altitude and equivalent airspeed profiles to low-level sorties. However, because the sorties were flown over the sea, the gust regime was relatively benign and this is illustrated in the wing stress and NZ plots.

Finally, the training sorties (Fig. 4(d)) were primarily pilot and pilot's assistant (co-pilot) training missions. These sorties generally contained a large number of roller landings; in the example presented here there were eight roller landings. Air tests were also included in this grouping as the profiles were similar.

## 5.0 TRAINING, INDEPENDENT VALIDATION SET AND IN-SERVICE DATA

The maximum expected structurally significant strain time history frequencies in the wing were considered likely to be less than 5-6Hz, based upon the average frequency content of wing data from larger and smaller aircraft. Therefore, all parametric and strain data were sampled at 64samples/s (minimum ten times the maximum frequency of interest) and 16Hz anti-aliasing filters were fitted to all

https://doi.org/10.1017/S0001924000002190 Published online by Cambridge University Press

channels. By using the same sample rate and filter settings for all data it was intended to minimise any phase shift differences or time lags between channels due to filtering. Twelve electrical resistance strain gauge full-bridges were located on the lower surface of the wings, along the 37·5% chord line of the wing, coincident with the front spar (illustrated in Fig. 5). Two bridges were located at each of the three stations (station W4, W5 and W6) on the port and starboard wing, either side of the critical feature location at that station. The outputs from each pair of bridges were combined to produce six channels (PW4, PW5, PW6, SW4, SW5 and SW6, where *P* represented the port wing and *S* represented the starboard wing). Locations PW5 and SW5 had been identified as the overall critical feature on the wing, from the damage tolerance analysis but the stress levels at locations W4 and W6 were sufficiently close theoretically that they were included in the instrumentation fit. Analysis of the data from the early sorties captured confirmed the theory and the port gauge (PW5) was chosen for this study because the average stress range in the port wing was found to be slightly higher than in the starboard wing; ground impact appeared to occur first on the port side more frequently than on the starboard side and location W5 was, as expected, more highly stressesd than locations W4 and W6. The analysis, using the strain gauge data for this programme, was undertaken in stress rather than strain. The units of stress used were consistent with the imperial units used in the design of the aircraft. Therefore, all stresses quoted in this paper are in lb force per square inch (psi), where 1psi = 6·895kPa.

Altitude, airspeed and outside air temperature data were captured from the ARINC 429-10 data bus on the aircraft; additional instrumentation including a normal accelerometer, positioned at the centre of gravity, and an inclinometer were also fitted to the aircraft. The inclinometer was used as a cost-effective method of obtaining an indication of aircraft bank angle. Additionally, signals were tapped from the aircraft weight-on-wheels micro switch and the No 2 engine-driven generator; the generator signal was used to trigger acquisition recording. All data were signal conditioned and recorded on an ACRA KAM-500 data acquisition unit. Although the data from the ARINC 429 data bus were sampled at 64samples/s, the data were only refreshed every 100ms or 50ms, depending upon the parameter; therefore, captured data were frequently stale. However, the altitude, airspeed and outside air temperature parameters did not fluctuate rapidly and a certain amount of padding of the data was considered acceptable. Ideally, a more extensive parameter set, including lateral acceleration, flap and aileron position, pitch and roll rates and pitch and roll accelerations would have been captured but the additional cost of capturing these parameters could not be justified within the programme. All flight data were subject to range and rate-of-change anomaly detection and data with significant anomalies were rejected (this only occurred on the normal acceleration channel for eight of the over 200 flights used in this study) and data with minor anomalies were replaced with the last known good value.

OLM data were divided into the four sortie-type groups and the maximum and minimum wing stress levels were identified for each flight and the associated fatigue damage for location PW5 was calculated from the stress time history, using Downing and Socie's rainflow cycle counting method[15,16] and a load-load transfer joint L65 aluminium alloy S-N curve from ESDU 89046[17] with a Goodman[18] mean-stress correction, with Miner's[19] sum to unity. It should be noted that a factor of 2·0 was applied to the stress levels of the PW5 output during the fatigue analysis process. This was to reflect a feature with a higher stress concentration factor than at the strain gauge location, such as at a notch feature and to ensure that a reasonable proportion of the smaller cycles in the time history were damaging and to exercise further the SHAUNN models. In all, 201 sorties were used in this analysis (20 for the training and testing of type specific models, 12 for independent validation, 165 for an in-service data set and seven for training a general model (includes four sorties from the type-specific training set)).

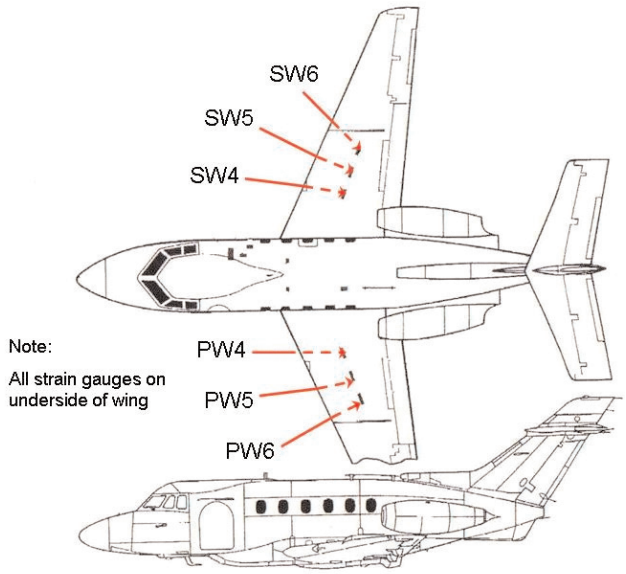



Figure 5. Dominie OLM wing strain gauge locations.

Sorties were selected by using stress range and maximum fatigue damage criteria, five sorties from each of the four sortie types were selected for training the models (20 sorties) and three sorties from each sortie type were identified as the independent validation set (IVS) (12 sorties). Also, to provide a control with which to assess the performance of the type-specific models, the seve most severe flights in the data set, using stress range and damage criteria were selected for use in training a General model, used as a control. Not surprisingly, these sevenflights were all drawn from Type 2 Low-level flying. They also included the four sorties in the Type 2 specific training data set but not the three IVS sorties for Type 2. The IVS for each of the type-specific models was used as the IVS for the General model, when used to predict each sortie data type. Therefore, for Type 2 data predictions, for example, the Type 2 IVS was used with the General model to generate expected values and confidence limits. Data not included as either training or IVS for any models was collated into a 165-flight in-service data set.

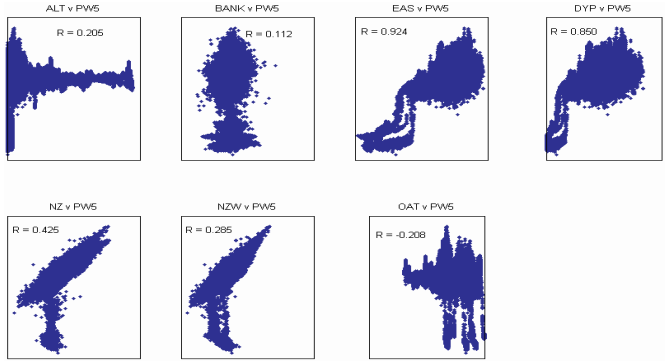
## 6.0 FLIGHT PARAMETER SELECTION

Domain knowledge was applied to the available input data set. Equivalent airspeed (EAS) was included as an input parameter and was also squared to produce a measure of dynamic pressure (DYP). The input data were normalised and hence the exclusion of constant values (i.e. the ½) was not significant. Additionally, normal acceleration (NZ) was conditioned by aircraft mass. However, fuel mass during the flight was not recorded and hence an algorithm was developed to estimate mass. The all-up (total) start-up and shut-down mass of the aircraft were manually recorded, as was the fuel mass at start and shut down. Therefore, standard fuel-burn data from the aircraft mission planning flight reference cards were used to estimate fuel burn during taxi out, taxi back, climb and descent. The time at the top of the climb for the flight was identified by moving forward through the flight from take off and using airspeed and altitude data to identify the top of the climb. Fuel burn, based upon climb rate, was calculated for the climb phase. A similar exercise, working backwards from final landing to the top of the descent, was undertaken. Thereafter a linear fuel burn from top of the climb to the start of descent was assumed and the total mass of the aircraft throughout the flight was

https://doi.org/10.1017/S0001924000002190 Published online by Cambridge University Press

**Table 1**
**Dominie wing stress mapping flight parameters**
**(Domain knowledge applied)**

| DOMINIE WING MAPPING FLIGHT PARAMETERS | | |
|---|---|---|
| SERIAL | PARAMETER | MEASURAND |
| 1 | ALT | Altitude |
| 2 | BANK | Inclinometer angle |
| 3 | EAS | Equivalent airspeed |
| 4 | DYP | Dynamic pressure |
| 5 | NZ | Normal acceleration |
| 6 | NZW | Normal acceleration * mass |
| 7 | OAT | Outside air temperature |
| 8 | WOW | Weight-on-wheels (discrete) |




Note: WOW not included as discrete value (0 or 1 only)

Figure 6. Input parameter correlation with wing stress (PW5) Type 2 training set.

**Table 2**
**Pearson correlation between Individual Input parameters and wing stress (PW5)**

| CORRELATION BETWEEN INPUT PARAMETERS AND TARGET FOR TRAINING SET DATA | | | | | | | | |
|---|---|---|---|---|---|---|---|---|
| TRAINING SET | ALT | BANK | EAS | DYP | NZ | NZW | OAT | WOW (Note 1) |
| Type 1 Civil | 0.336 | 0.130 | 0.926 | 0.819 | 0.261 | 0.004 | -0.356 | N/A |
| Type 2 Low-Level | 0.205 | 0.112 | 0.924 | 0.850 | 0.425 | 0.285 | -0.208 | N/A |
| Type 3 Maritime | 0.290 | 0.197 | 0.935 | 0.828 | 0.271 | 0.001 | -0.284 | N/A |
| Type 4 Training | 0.433 | 0.213 | 0.910 | 0.809 | 0.451 | 0.305 | -0.470 | N/A |
| General | 0.328 | 0.141 | 0.949 | 0.886 | 0.361 | 0.191 | -0.321 | N/A |
| **AVERAGE** | **0.318** | **0.159** | **0.929** | **0.838** | **0.354** | **0.157** | **-0.328** | **N/A** |
| Note 1: WOW is a discrete value (0 or 1) and hence correlation was not considered applicable | | | | | | | | |

calculated from these data. This process was validated against a Type 1 – Civil Transport flight in which the aircrew had recorded fuel mass periodically during the flight and good agreement was achieved (within 2% of all-up mass). It was accepted that this method would be less accurate for Type 2, 3 and 4 sorties, due to their more complex profiles, but a significantly more complex algorithm could not be justified or validated, particularly when the accuracy of the fuel gauging system was +/- 180lb per wing. As a precaution against inaccuracies in this algorithm, normal acceleration, as well as normal acceleration conditioned by mass, was included within the parameter set. The full input parameter set is presented in Table 1.

The training sets were optimised towards the extremes of tensile and compressive stress (i.e. more data points were selected from the extremes of tensile and compressive stress than from mid-range data points). Additionally, the IVS for each sortie type were generated by concatenating the 3 flights of each type and taking every second point in the data stream, otherwise the files became excessively large. Each training set consisted of over 300,000 examples of each input parameter.

## 7.0 PARAMETRIC DATA TO STRAIN CORRELATION

The Pearson correlation coefficients[21] between the individual input parameters and the wing stresses for all training sets were calculated and are reproduced in Table 2. The airspeed parameters (EAS and DYP) exhibited far higher correlations than the normal acceleration parameters (NZ and NZW) although, the NZ correlations were a little higher for the more severe flying (Type 2 and Type 4). An example correlation plot, for the Type 2 training data set is re-produced in Fig. 6.

It is noteworthy that the correlation coefficients for the mass conditioned normal acceleration (NZW) were lower than the normal acceleration parameter (NZ) across all training data sets. This could have been partly attributable to the approximate method of generating mass data. However, analysis of the variation in wing stress with fuel mass, from data captured during ground-borne sortie phases, had identified that the relationship was non-linear and this would have reduced the correlation coefficient further.

## 8.0 MODEL TRAINING

Three models were trained for each of the four sortie-type and the general data sets. All models had a single hidden layer of 25 logistic sigmoid neurons, with a learning rate of 0·1 and a momentum coefficient of 0·5. Twenty-five neurons in the hidden layer had proven adequate to capture the parameter-to-stress or strain relationships in previous studies and this was close to the 19 neurons suggested by Kolmogorov's[21] theorem for nine inputs (2*inputs+1). Half of each input data set was used for model training and half was used as the test set. The mean squared error of the training set was calculated after every weight update (over 150,000 times per epoch) and the test mean squared error was calculated after each epoch. Training was undertaken for 2,000 epochs; preliminary runs had shown the gradient of the training mean squared error to be extremely small by 2,000 epochs (<<0·1% change per epoch). The risk of over fitting was considered low due to the large size of training set and the IVS testing procedures in place. All models produced consistent results with stable training; the test set correlation coefficients between predicted and target stresses were in the range 0·997 to 0·999 for all models.

https://doi.org/10.1017/S0001924000002190 Published online by Cambridge University Press

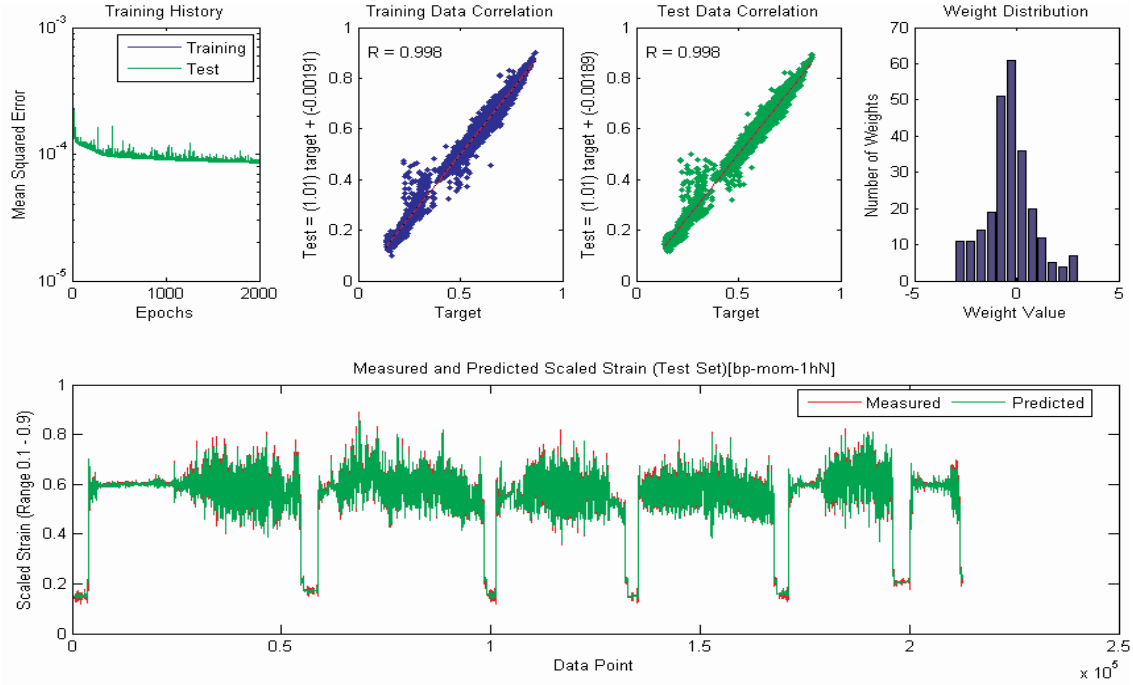



Figure 7. Training environment plot type 2 run3 model.

**Table 3**
**Comparison of target, predicted and expected maximum and minimum stress**

| PREDICTED MAXIMUM AND MINIMUM VALUES AND ASSOCIATED TARGET VALUES - CHOSEN MODELS | | | | | | | |
|---|---|---|---|---|---|---|---|
| MODEL | TARGET MAXIMUM STRESS (psi) | PREDICTED MAXIMUM STRESS (psi) | MAXIMUM STRESS RATIO PREDICTED / TARGET | TARGET MINIMUM STRESS (psi) | PREDICTED MINIMUM STRESS (psi) | MINIMUM STRESS RATIO PREDICTED / TARGET | DAMAGE RATIO PREDICTED / TARGET |
| Type 1 Run 2 | 9956 | 9746 | 0.98 | -3910 | -3249 | 0.83 | 0.64 |
| Type 2 Run 3 | 12125 | 12479 | 1.03 | -3818 | -3429 | 0.90 | 0.88 |
| Type 3 Run 1 | 9786 | 9631 | 0.98 | -3583 | -3289 | 0.92 | 0.75 |
| Type 4 Run 1 | 9673 | 9493 | 0.98 | -2946 | -2778 | 0.94 | 0.93 |
| Gen Type 1 Run 3 | 9956 | 9927 | 1.00 | -3910 | -3618 | 0.93 | 0.71 |
| Gen Type 2 Run 3 | 12125 | 11951 | 0.99 | -3818 | -3621 | 0.95 | 0.81 |
| Gen Type 3 Run 2 | 9786 | 9372 | 0.96 | -3583 | -3344 | 0.93 | 0.70 |
| Gen Type 4 Run 3 | 9673 | 9816 | 1.01 | -2946 | -2646 | 0.90 | 0.80 |
| **Average** | | | **0.99** | **Average** | | **0.91** | **0.78** |

| EXPECTED MAXIMUM AND MINIMUM VALUES AND ASSOCIATED TARGET VALUES - CHOSEN MODELS | | | | | | | |
|---|---|---|---|---|---|---|---|
| MODEL | TARGET MAXIMUM STRESS (psi) | EXPECTED MAXIMUM STRESS (psi) | MAXIMUM STRESS RATIO EXPECTED / TARGET | TARGET MINIMUM STRESS (psi) | EXPECTED MINIMUM STRESS (psi) | MINIMUM STRESS RATIO EXPECTED / TARGET | DAMAGE RATIO EXPECTED / TARGET |
| Type 1 Run 2 | 9956 | 9759 | 0.98 | -3910 | -3360 | 0.86 | 0.65 |
| Type 2 Run 3 | 12125 | 12369 | 1.02 | -3818 | -3500 | 0.92 | 0.87 |
| Type 3 Run 1 | 9786 | 9636 | 0.98 | -3583 | -3117 | 0.87 | 0.72 |
| Type 4 Run 1 | 9673 | 9612 | 0.99 | -2946 | -2725 | 0.92 | 0.93 |
| Gen Type 1 Run 3 | 9956 | 9622 | 0.97 | -3910 | -3578 | 0.92 | 0.71 |
| Gen Type 2 Run 3 | 12125 | 11821 | 0.97 | -3818 | -3637 | 0.95 | 0.79 |
| Gen Type 3 Run 2 | 9786 | 9317 | 0.95 | -3583 | -3141 | 0.88 | 0.66 |
| Gen Type 4 Run 3 | 9673 | 9469 | 0.98 | -2946 | -2536 | 0.86 | 0.70 |
| **Average** | | | **0.98** | **Average** | | **0.90** | **0.75** |

https://doi.org/10.1017/S0001924000002190 Published online by Cambridge University Press

**Table 4**
**Summary of dominie wing models performance with in-service data set**

| SUMMARY OF DOMINIE WING MODEL PERFORMANCE WITH IN-SERVICE DATA SET | | | | | | | | | | |
|---|---|---|---|---|---|---|---|---|---|---|
| MODEL TYPE | NUMBER OF FLIGHTS IN TYPE | PREDICTED STRESS CORRELATION COEFFICIENT | EXPECTED STRESS CORRELATION COEFFICIENT | TARGET MICRO DAMAGE | PREDICTED MICRO DAMAGE | EXPECTED MICRO DAMAGE | 95% CONFIDENCE MICRO DAMAGE | DAMAGE RATIO PREDICTED / TARGET | DAMAGE RATIO EXPECTED / TARGET | DAMAGE RATIO 95%CONF / TARGET |
| Type1 | 80 | 0.998 | 0.998 | 2889 | 2530 | 2847 | 2998 | 0.876 | 0.985 | 1.038 |
| GenType1 | 80 | 0.995 | 0.995 | 2889 | 2903 | 2817 | 3380 | 1.005 | 0.975 | 1.170 |
| Type2 | 49 | 0.997 | 0.997 | 6557 | 5961 | 5974 | 6665 | 0.909 | 0.911 | 1.016 |
| GenType2 | 49 | 0.998 | 0.998 | 6557 | 5830 | 5707 | 6231 | 0.889 | 0.870 | 0.950 |
| Type3 | 8 | 0.998 | 0.998 | 311 | 288 | 302 | 331 | 0.925 | 0.971 | 1.062 |
| GenType3 | 8 | 0.998 | 0.998 | 311 | 264 | 270 | 295 | 0.849 | 0.869 | 0.948 |
| Type 4 | 28 | 0.997 | 0.997 | 1532 | 1408 | 1481 | 1703 | 0.919 | 0.967 | 1.112 |
| GenType4 | 28 | 0.997 | 0.997 | 1532 | 1414 | 1297 | 1523 | 0.923 | 0.847 | 0.994 |
| **Type Total** | **165** | **0.998** | **0.998** | **11290** | **10187** | **10604** | **11696** | **0.902** | **0.940** | **1.148** |
| **Gen Total** | **165** | **0.996** | **0.996** | **11290** | **10411** | **10092** | **11428** | **0.922** | **0.894** | **1.012** |

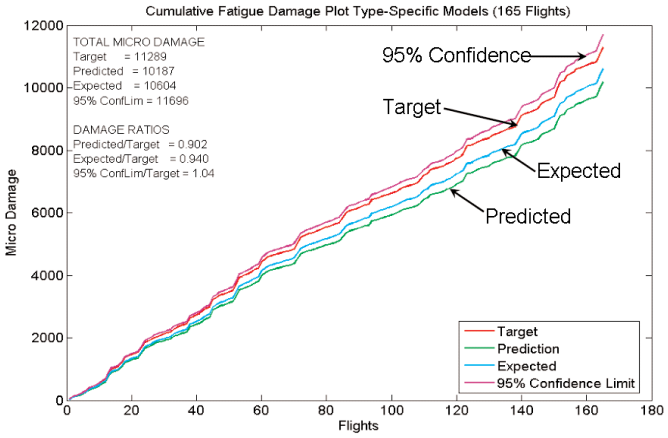



Figure 8. Cumulative damage predictions – in-service data type-specific models.

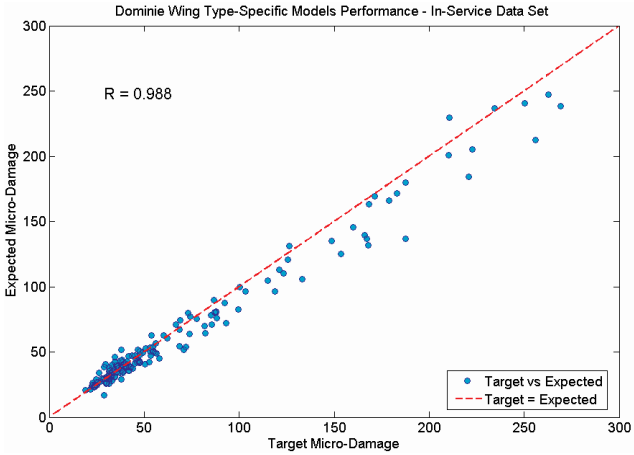



Figure 9. Flight-by-flight damage – In-service data – type-specific models.

## 9.0 INDEPENDENT VALIDATION

Independent validation of the models and confidence limits were calculated using Jepson *et al*'s[22] linear regularisation and cross-validation process. Expected stress values and 95% confidence limit values were generated for each prediction. Each Type-specific model had its own IVS, from the same sortie grouping, and the General model was tested against each IVS in turn, to provide a comparison with the Type-specific model. All models achieved a high level of stress correlation with coefficients for the IVS ranging from 0·996 to 0·998. Additionally, the gradient of the best-fit lines were generally close to 1·0 and the best-fit axis intercepts (offsets) were small. However, generally the models significantly underestimated the fatigue damage for the IVS. The reasons for this were investigated and this quickly focused on the prediction of the stresses seen when the aircraft was on the ground. It was evident from the training environment plots that the models had generally captured the stresses for airborne segments of the sortie and were capturing the mean stress on the ground but not the fluctuation about that mean stress; an example training environments, from Type 2 Run3, is reproduced in Fig. 7.

Thereafter, a more detailed investigation into the prediction of ground-borne sortie phases was undertaken. For each model, the maximum and minimum stress in the IVS was identified and the corresponding maximum and minimum model predicted and expected stresses were identified. The maximum or minimum predicted and expected values over a small time window around the target maximum and minimum value were used to ensure corresponding peak data were captured. These data are reproduced in Table 3.

It was evident that the maximum stress was generally well predicted by the models; the Type-specific model predicted and expected values of the maximum stress were all within 3% of the target value and the General model was within 5% of this value, for all IVS data sets. However, for the minimum stress, the predicted and expected values from the models were up to 17% in error and always under predictions. Therefore, to correct this under-prediction for assessment of performance against in-service data, the expected values for all compressive (negative) stresses were divided by the expected / target ratio in Table 3, appropriate to the model.

## 10.0 MODEL PERFORMANCE WITH IN-SERVICE DATA

The performance of the four Type-specific models and the General model were tested using the 165-flight in-service data set. The Type-specific models were tested against data from the corresponding sortie type and the General model was tested against all data but with the expected values corrected using the factors appropriate to each type of sortie (i.e. 'tuned' to the data type). OLM data were only captured for one aircraft and therefore it was not possible to

https://doi.org/10.1017/S0001924000002190 Published online by Cambridge University Press

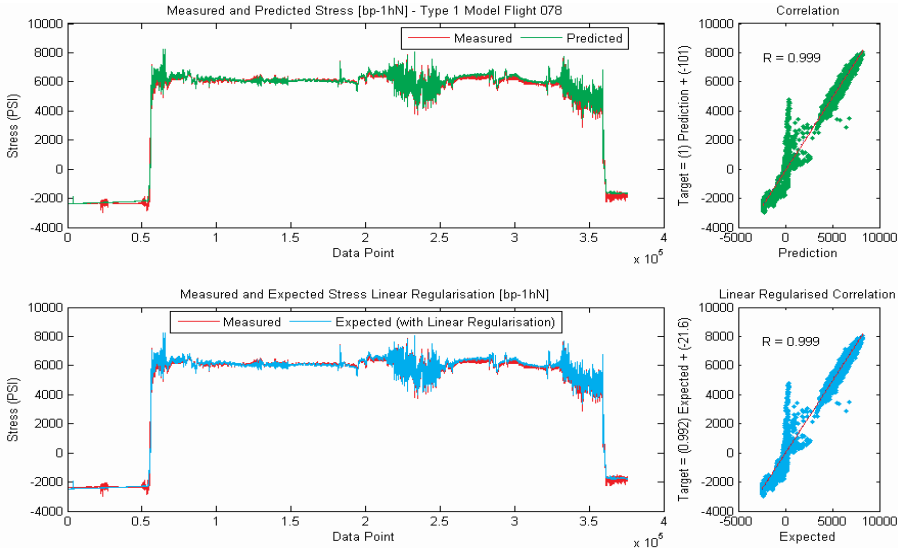



Figure 11. Predicted and expected stress high correlation type 1 model flight 078.

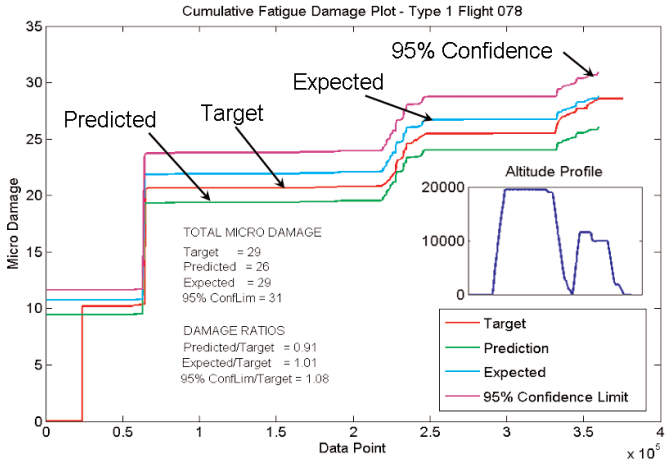



Figure 12. Predicted, expected and 95% confidence damage plot flight 078.

demonstrate applicability of the models across more than one aircraft. Data are presented by sortie type and the predicted and expected correlation coefficients, and the fatigue damage accrual for predicted, expected and 95% confidence limit data are identified. The 95% confidence limit fatigue damage was calculated using the upper 95% confidence tensile stresses and the lower 95% confidence limit compressive stresses to give the maximum stress range for each cycle. A summary of performance of the models over the 165 flight in Service data set is detailed in Table 4.

From the above data, it was evident that all models had captured the underlying relationships between parameters and stresses. Over 165 flights of unseen data, the average stress correlation for the Type-specific models was 0·998 and for the General model was 0·996. On average, the damage calculated from Type-specific model stress predictions was 9·8% below the target value and the damage from the expected stress was 6·0% below target. For the General model the damage calculated from predicted stress was 7·8% below the target value and the damage from the expected stress was 10·6% below target. This means that for the General model the correction applied to the predicted stress using the best-fit line had a greater

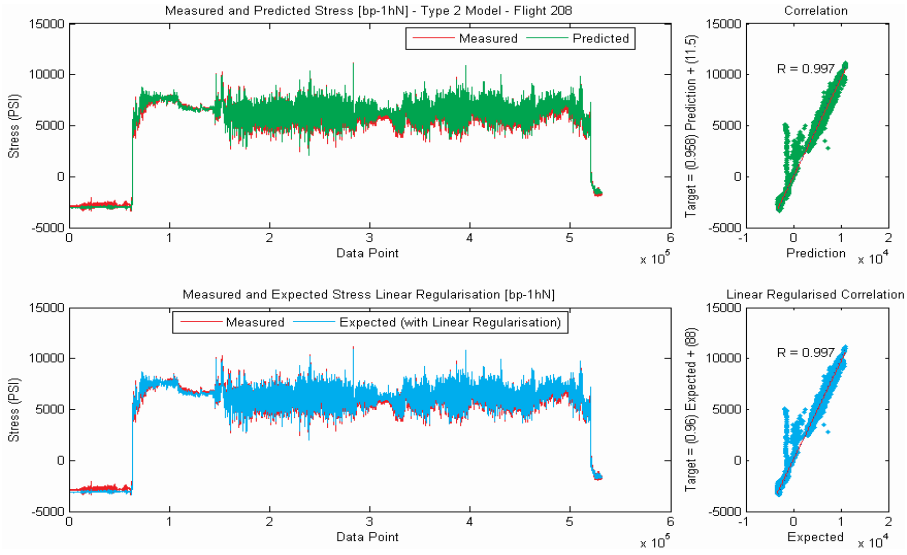



Figure 13. Predicted and expected stress severe flight type 2 model flight 208.

https://doi.org/10.1017/S0001924000002190 Published online by Cambridge University Press

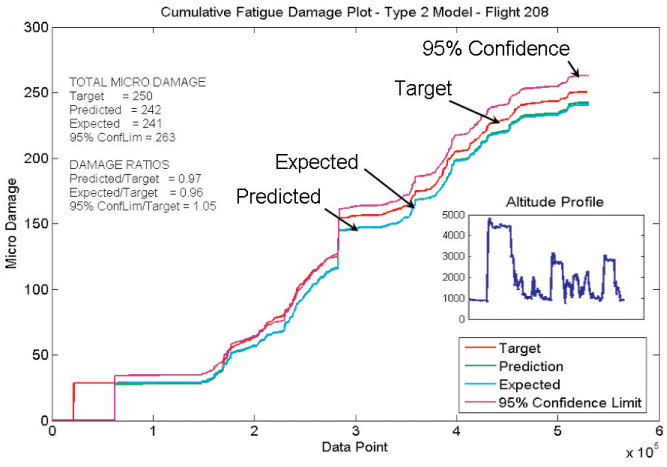



Figure 14. Predicted, expected and 95% confidence damage plot flight 208.

influence than the compressive stress correction on the damage calculated. The cumulative fatigue damage prediction for the in-service data for the Type-specific models are presented graphically in Fig. 8 and plots of the performance of the models on a flight-by-flight basis are reproduced in Fig. 9 respectively.

The fatigue damage flight-by-flight correlation, for the 165-flght in-service data set was 0·988 for the Type-specific models and 0·986 for the General model. In order to provide some comparison of the scatter in performance of the SHAUNN models with current in-use systems, a plot of the fatigue index calculated for the in-service data set, using the fatigue meter accelerometer recordings and the Dominie fatigue meter formula[23], against fatigue damage at the wing critical location is reproduced in Fig. 10. It is evident that the flight-by-flight damage correlation from current methods ($R$ = 0·460 for the 165-flight in-service data set) is significantly lower than obtained from the SHAUNN models.

As well as investigating the damage sum on a flight-by-flight basis, the predicted, expected and 95% confidence limit stress and the associated through-sortie damage accrual were analysed for each flight in the in-service data set. Examples from two flights are reproduced here. In Fig. 11 the predicted and expected stresses are plotted against target values for a Type 1 – Civil Transport flight, Flight 078, with a high stress correlation coefficient ($R$ = 0·999). The corresponding damage plot is produced in Fig. 12. Figures 13 and 14 provide the same data for a below average correlation flight (Flight 208, $R$ = 0·997), which was a severe Type 2 – Low-Level flight.

The stress correlations were high in all the tests using the in-service data set; however, a region of the flight in each target against predicted or expected stress cross plot was identified as being poorly correlated (this was particularly evident in Flight 078 (Fig. 11). Further investigation revealed that this loss of correlation was due to local poor predictions and a time lag in the prediction of stress during the landing and take-off phases. This is illustrated in Fig. 15, where the take-off and landing phases of Flight 078 are shown in close up. The lag during take-off and the apparent spike in the prediction during landing were primarily a result of the weight-on-wheel (WOW) micro switch changing state. During the take-off phase a rapid change in predicted stress was noted at approximately 55,530 data points and this was confirmed as corresponding to the micro switch state change. During the landing phase, the apparent data spike also coincided with the micro switch state change from airborne to on-ground. These anomalies backed up the desire not to use discrete inputs directly; however, overall model accuracy suffered significantly when the weight-on-wheels indication was removed from the data set. Therefore, in the absence of a scalar method of differentiating between airborne and ground phases, the WOW data were retained.

The predicted and expected damage plots (Fig. 12 and Fig. 14) followed the target damage accrual well throughout most of the flight. However, there were noticeable differences in the early phases of the flight and this was particularly apparent in the relatively benign Type 1 flights (Fig. 12). This was caused by the models being unable to capture the fluctuations of stress when the aircraft was on the ground. The minimum predicted stress value generally occurred at start up, when the aircraft was heaviest. However, target minimum values, due to stress fluctuations about the mean, often occurred just before take-off during the run up against brakes and this fluctuation was not predicted by the models. Therefore, in the rainflow algorithm the predicted GAG cycle minimum cycle was often right at the beginning of the flight, whereas the target minimum value was just before take-off. This cycle pairing difference was then apparent in the damage accrual plots.

Notwithstanding these issues, the correlation between expected stress and target values, produced from both the Type-specific and General models was above the initial target of 0·995; also, the corresponding damage accrual for the in-service data set was within the initial aim of within +/-10% of the target damage. The Type-specific models produced marginally more accurate expected values than the General model and hence the Type-specific model data were used for the confidence limit, novel input data, sensitivity and significance analysis work, described in the following sections.

## 11.0 NOVELTY DETECTION

Where possible SHAUNN-type models should be used to interpolate within the training experience rather than extrapolate outside it. However, it is reasonable to assume that in-service data will contain values not covered by the experience of the training set. Exceedences of training data input parameter limits can be clearly identified by deterministic methods. However, data within the extremes of the training set can lie in poorly or unpopulated regions within the multidimensional input space and identification of this occurrence can be problematic. If the majority of the variance in the input data set can be captured in the 1st and 2nd principal components[20] of input parameters, then this method can be used as a guide to identifying possible novel input data by overlaying new input data on top of projected components of the training data set. For the 4 Type-specific data sets, between 75·4% and 82·7% of the variance in the data was contained within the 1st and 2nd principal components; this is illustrated in Fig. 16.

Principal Component Analysis (PCA) projections for each IVS data set or in-service sortie were produced and compared with the projections for the training set for each type of sortie. Only Flight 180 (Fig. 17) of the 165-flight in-service data set was identified as having input data outside of the projection of the relevant training set and this was investigated further.

The apparent novel data identified in Flight 180 (Fig. 17) (a Type 3 flight) was isolated. The apparent novel data points identified were found to coincide with a section of high-altitude flying (Fig. 18), during which the altitude recorded was marginally greater than seen in the maritime sortie training data set but just inside the margin allowed in the limits and hence an exceedence was not triggered. Although the intention should be to use SHAUNN models to interpolate rather than extrapolate, if a good generalised model had been produced it would be expected to be able to accommodate such small excursions outside of training experience. To investigate the performance of the model in the novel region, the stress prediction plots for the whole flight and the region of interest were plotted (Fig. 19). Although the predictions for the novel-data region had an error in this region of 700 psi, there was no noticeable change in this error between predictions in the vicinity of these data marginally within the training experience and those marginally outside the experience.

https://doi.org/10.1017/S0001924000002190 Published online by Cambridge University Press

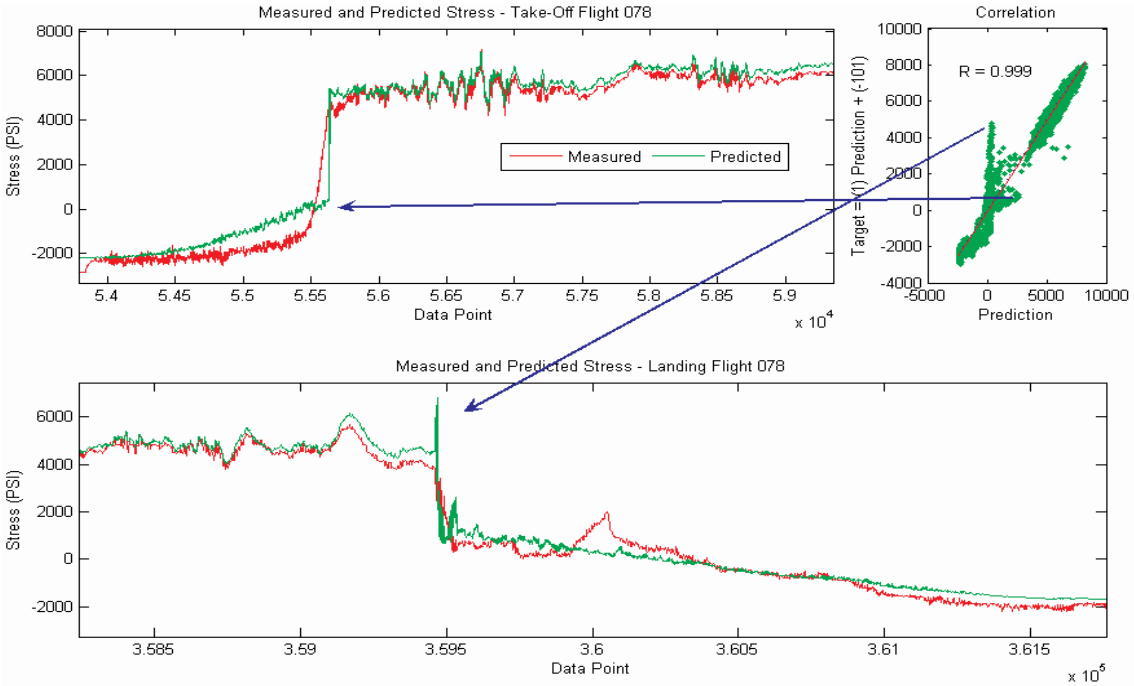



Figure 15. Take-off and landing phases – flight 078.

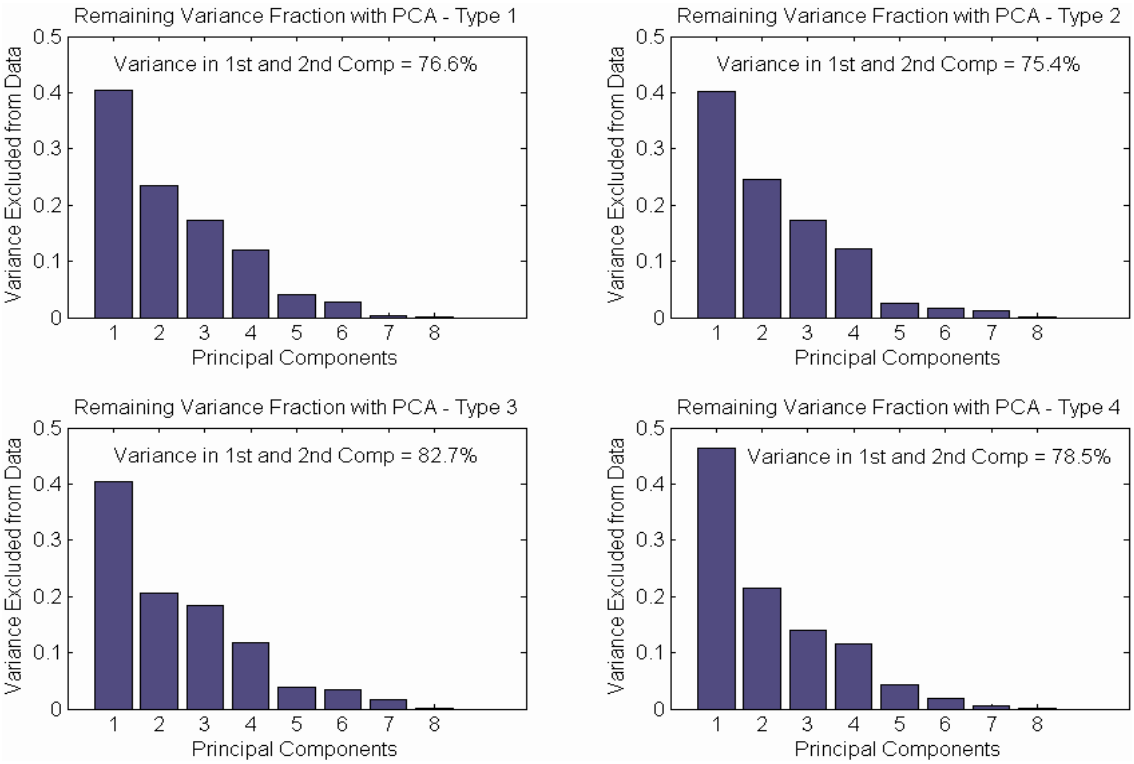



Figure 16. Variance fraction lost with principal components – type1-4 data sets.

https://doi.org/10.1017/S0001924000002190 Published online by Cambridge University Press

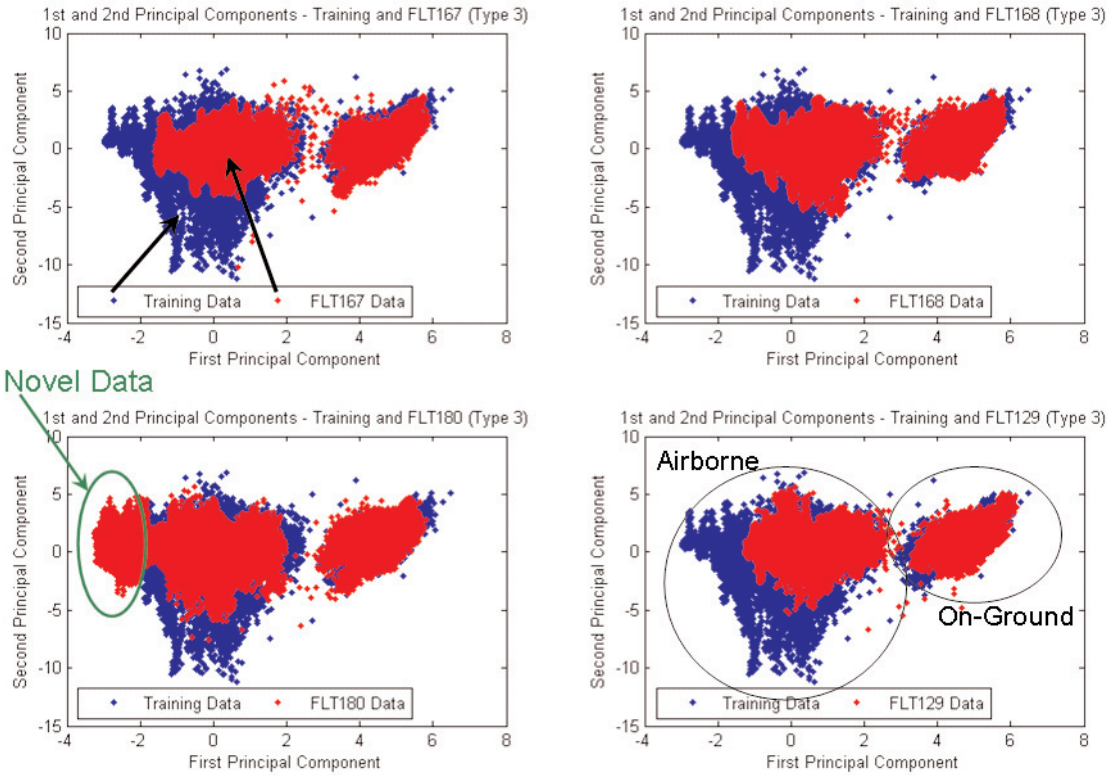



Figure 17. Example 1st and 2nd principal component plots type 3 flights.

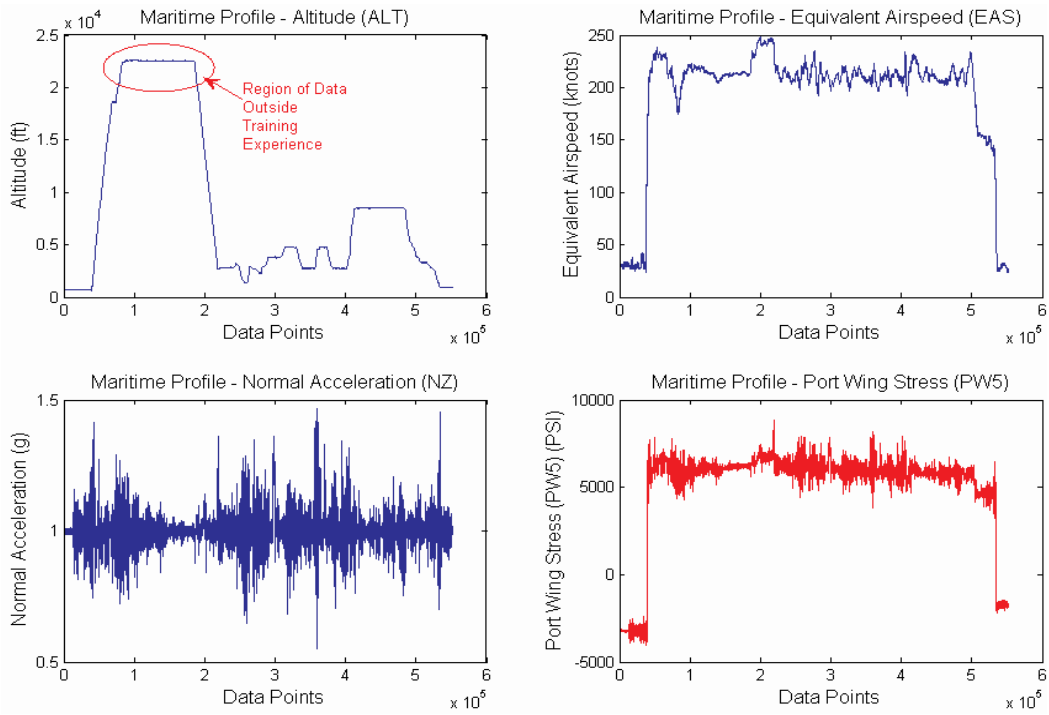



Figure 18. Flight 180 – ALT, EAS, NZ and PW5 stress plots.

https://doi.org/10.1017/S0001924000002190 Published online by Cambridge University Press

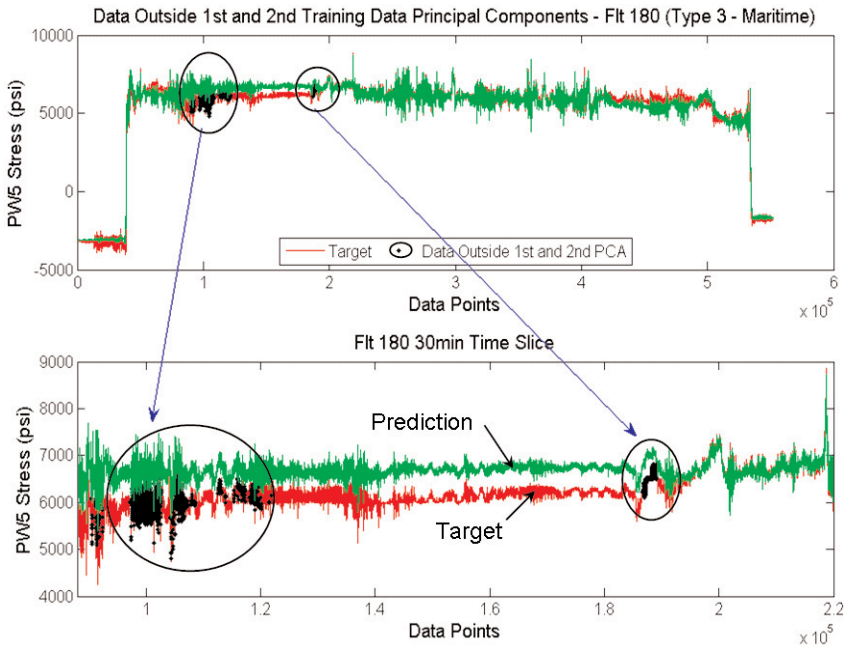



Figure 19. Data outside 1st and 2nd principal components flights 180 stress prediction.

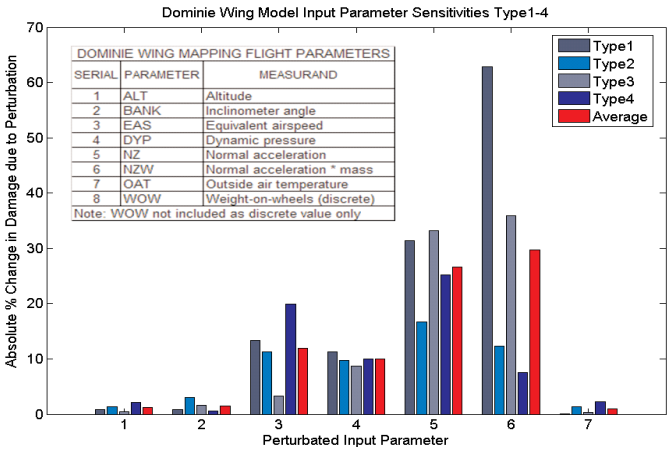



Figure 20. Sensitivity analysis dominie wing data.

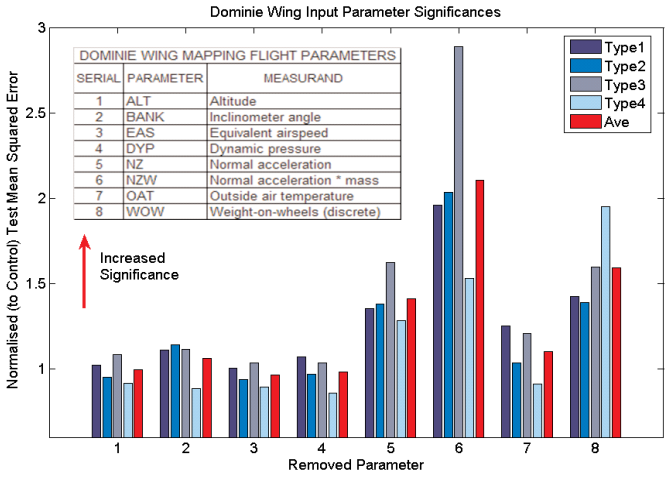



Figure 21. Dominie wing Input parameter significances type 1-4 models.

## 12.0 SENSITIVITY ANALYSIS

Sensitivity analysis, based upon a small perturbation method described by Tsoukalas and Uhrig[21] was undertaken. The IVS data for each of the Type-specific models was used as input and each parameter was incremented and decremented by 5%. From these values, the average damage change between the original and data subject to perturbation was calculated for each input and for each Type-specific model. Thereafter, input parameters were ranked in sensitivity order, based upon the absolute average damage change for the four Type-specific models. The results from this investigation are reproduced in Fig. 20. Generally, models were more sensitive to perturbations in the normal acceleration parameters (NZ and NZW) than the remaining input parameters. Models with smaller variations in normal acceleration parameters in their training data (Type 1 – Civil Transport and Type 3 – Maritime) were more sensitive to the perturbations in these parameters.

## 13.0 INPUT PARAMETER SIGNIFICANCES

The input parameter significances were identified by removing each of the eight input parameters in turn and training the 7-input parameter models for 100 epochs of the relevant training data set, using a learning rate of 0·1 and a momentum coefficient of 0·5. Models were trained for each removed parameter for each of the 4 Type-specific training sets and test mean squared error at the end of training were recorded for the 32 models generated. Models were then ranked, using the increase in test mean squared error as a result of removing each parameter. This measure was used to identify the relative significance of the input parameters. The results are presented graphically in Fig. 21.

The ranking of input parameter significances was very consistent across the models. Mass conditioned normal acceleration (NZW) was the most significant input parameter, despite this parameter having a low correlation with the stress time history, in the range 0·001 to 0·305 for the training data (Table 2). This high significance

https://doi.org/10.1017/S0001924000002190 Published online by Cambridge University Press

is apparent because although the normal acceleration parameters (NZW and NZ) did not correlate well with the mean stress value, they did correlate with the fluctuation about that mean stress. All models identified NZW as more significant than NZ (which was the 3rd most significant parameter); this implied that although the mass estimation algorithm did have its limitations, it did improve the performance of the model. The second most significant parameter was the weight-on-wheels discrete value (WOW). Its significance varied considerably between models, with the peak significance value occurring in the Type 4 (Training) model. This was because the training data set for the Type 4 models had far more roller landings than any of the other data sets. The models evidently needed the WOW input to map the significant change in stress in the wing associated with the take-off and landing phases.

## 14.0 SHAUNN SYSTEM IMPLEMENTATION

OLM programmes are mandated[24] for UK military fixed-wing aircraft and hence the controlled prime data needed to develop SHAUNN-based monitors would be captured by extant programmes. Some small changes to parametric data sets might be needed to develop a SHAUNN monitor for a particular structural locations but the additional burden to the OLM programme would be relatively small in comparison. Therefore, where service lives of structurally significant features are limited by either inaccurate monitoring, and hence attract additional conservatism in the monitoring system, or where there is no structural usage monitoring currently, then implementation of SHAUNN-based parametric monitors could provide more cost-effective solutions than early retirements, modifications or increased structural inspections.

Once the SHAUNN algorithms had been trained, tested and certified (discussed at length in Reed[13]), using the process for non-adaptive predictive methods detailed in UK Defence Standard 00-970[25], the burden on operators would be relatively small. Modern data acquisition systems have sufficient memory capacity to allow download when maintenance activity allowed, weekly for example, and rapid semi-automated processing of data through the SHAUNN algorithms in a ground station would be only a small burden to maintenance operators.

## 15.0 CONCLUSIONS

The data generated within this study clearly illustrated the potential for the use of SHAUNN-based models for aircraft fatigue and usage monitoring systems by mapping flight parameters to stresses, strains or loads and the following conclusions were drawn from this work:

- Relatively simple single layer MLP ANN models were trained using sequential back-propagation with momentum, with a very limited input parameter data set. These models were able to predict the stresses in the wing of an RAF Dominie aircraft with an average correlation coefficient of 0·998 over 165 flights of unseen data (81 million data points); this was within the aim of an average correlation coefficient of 0·995.
- The predicted fatigue damage for the 165-flight in-service data set was 9·8% under target and the expected damage was 6·0% under target. This is within the monitoring system design aims of +/-10%.
- Models trained using 4 different sortie types of: Type 1 – Civil Transport, Type 2 Low-level, Type 3 – Maritime and Type 4 – Training sorties, produced slightly more accurate results, in stress correlation and damage terms, than a General model for all types of flying ($R$ = 0·996 and expected damage –10·6%).
- The fatigue damage flight-by-flight correlation, for the 165-flght in-service data set was 0·988 for the Type-specific models and 0·986 for the General model. This represented a significant improvement over the current fatigue monitoring system for the Dominie which produced a flight-by-flight damage correlation coefficient of 0·460 for the 165-flight in-service data set.
- The parametric data set did not include fuel mass and consequently this had to be estimated. However, the effect of mass variation on wing stresses for the Dominie aircraft was highly significant and automated fuel mass recording and mass distribution data would be required for further model enhancement.
- The wing fatigue damage accrual for the Dominie aircraft is dominated by the ground-air-ground cycle. Consequently, the failure of the models to capture the stress fluctuations on the ground about the mean stress value was significant. Further work to improve the parameter set to enable these stress fluctuations to be mapped, such as investigating filtering and amplifying elements of the parametric signals or investigating the use of wing-tip accelerometers, should be undertaken.
- Between 75·4% and 82·7% of the variance in the input data was contained within the 1st and 2nd principal components (depending on the model type) and these data were used to provide a guide for novel input data outside of the training experience. Only one minor region of novel data was identified and the model performance was not seen to degrade significantly due to the input of marginally novel data.
- Generally, models were more sensitive to perturbations in the normal acceleration parameters (NZ and NZW) than the other input parameters. Models with smaller variations in normal acceleration parameters in their training data (Type 1 – Civil Transport and Type 3 – Maritime) were more sensitive to the perturbations in these parameters.
- The ranking of input parameter significances was very consistent across the models. Mass conditioned normal acceleration (NZW) was the most significant input parameter, this was despite this parameter having a low correlation with the stress time history, in the range 0·001 to 0·305 for the training data. This high significance was apparent because although the normal acceleration parameters (NZW and NZ) did not correlate well with the mean stress value, they did correlate with the fluctuation about that mean stress.
- All models identified NZW as more significant than NZ (which was the 3rd most significant parameter); this implied that although the mass estimation algorithm did have its limitations, it did improve the performance of the model. The second most significant parameter was the weight-on-wheels discrete value (WOW). Its significance varied considerably between models, with the peak significance value occurring in the Type 4 (Training) model. This was because the training data set for the Type 4 models had far more roller landings than any of the other data sets. The models evidently needed the WOW input to map the significant change in stress in the wing associated with the take-off and landing phases.
- Areas for further investigation include stress predictions for empennage, fuselage and undercarriage structure stresses on similar and larger military transport aircraft in a variety or roles.

## ACKNOWLEDGEMENT

The author wishes to acknowledge QinetiQ Farnborough and the UK Ministry of Defence for giving permission to publish this work.

https://doi.org/10.1017/S0001924000002190 Published online by Cambridge University Press

## REFERENCES


1. HUNT, S.R. and HEBDEN, I.G. Eurofighter 2000: An Integrated Approach to Structural Health and Usage Monitoring, AGARD RTO Proceedings 7, Exploitation of Structural Loads/Health Data for Reduced Life Cycle Costs, Brussels, Belgium, 1998.
2. AZZAM, H. A practical approach for the indirect prediction of structural fatigue from measured flight parameters. Proceedings of the Institution of Mechanical Engineers, Part G: *J Aerospace Engineering*, **211**(G1), pp 29-38, 1997.
3. AZZAM, H., HEBDEN, I., GILL, L., BEAVEN, F. and WALLACE, M. Fusion and decision making techniques for structural prognostic health management, IEEE Aerospace Conference Paper #1535, 2005.
4. WALLACE, M., AZZAM, H. and NEW, S. Indirect approaches to individual aircraft structural monitoring, Proceedings of the Institution of Mechanical Engineers, **218**, Part G, *J Aerospace Engineering*, 2004, pp 329-346.
5. JACOBS, J.H. and PEREZ, P. A combined approach to buffet response analysis and fatigue life prediction, NATO AGARD Report 797 – An assessment of fatigue damage and crack growth prediction techniques, Papers presented at the 77th Meeting of the AGARD Structures and Materials Panel, Bordeaux, France, 29-30 September 1993.
6. KIM, D. and MARCINIAK, M. A methodology to predict the empennage in-flight loads of a general aviation aircraft using backpropagation neural networks, DOT/FAA/AR-00/50, Washington DC, USA, February 2001.
7. HILL, K., HUDSON, R.A., IRVING, P.E. and VELLA, A.D. Loading spectra, usage monitoring and prediction of fatigue damage in helicopters. Proceedings of the 18th ICAF Symposium on Aeronautical Fatigue, May 1995, Melbourne, Australia.
8. MANRY, M.T., HSIEH, C.H. and CHANDRASEKAREN. H. Near-optimal flight load synthesis using neural networks. Proceedings of the IEEE Workshop on Neural Networks for Signal Processing, Madison, Wisconsin, USA, August 1999.
9. LEVINSKI, O, Prediction of buffet loads using artificial neural networks, Document DSTO-RR-0218, Australian Defence Science and Technology Organisation, September 2001.
10. WANG, J. Service loads prediction and recorder data validation using artificial neural networks, PhD Dissertation, Institute of Aeronautics and Astronautics, National Cheng Kung University, Taiwan, July 2003.
11. REED, S.C. and COLE, D.G. Development of a parametric aircraft fatigue monitoring system using artificial neural networks, in Proceedings of the 22nd Symposium of the International Committee on Aeronautical Fatigue, 2003, Lucerne, Switzerland, ISBN 0954345428, Editor: GUILLAUME, M. (Ed).
12. REED, S.C. A parametric-based empennage fatigue monitoring system using artificial neural networks, in Proceedings of the 23rd Symposium of the International Committee on Aeronautical Fatigue, Hamburg, Germany, 2005.
13. REED, S.C. Development of a parametric-based indirect aircraft structural usage monitoring system using artificial neural networks, *Aeronautical J*, April 2007, **111**, (1118), pp 209-230.
14. HAYKIN, S. *Neural Networks: A Comprehensive Foundation*, 2nd Edition, Prentice Hall, 1999, ISBN 0-13-273350-1.
15. DOWNING, S.D. and SOCIE, D.F. Simple rainflow counting algorithms, *Int J Fatigue*, 1982, pp 31-40.
16. ASTM, Standard practices for cycle counting in fatigue analysis, American Society for Testing of Materials, E1049-85 (Re-approved 1997).
17. ESDU, Engineering Sciences Data Unit – Item 89046 – Fatigue of aluminium alloy joints with various fastener systems. Low load transfer, 1989.
18. GOODMAN, J. *Mechanics Applied to Engineering*, London, UK, Longmans Green, 1899.
19. MINER, M.A. Cumulative damage in fatigue, *J Applied Mechanics*, 1945, **12**, pp 159-64.
20. MANLY, B.F.J. *Multivariate Statistical Methods – A Primer*, Chapman and Hall CRC Press, Florida, USA, 2nd ed, ISBN 0-412-60300-4, 1994.
21. TSOUKALAS, L.H. and UHRIG, R.E. Fuzzy and neural approaches in Engineering, John Wiley and Sons Inc, ISBN 0-471-16003-2, pp 238, 1996.
22. JEPSON, B., COLLINS, A. and EVANS, A. Post-Neural Network Procedure to Determine Expected Prediction Values and Their Confidence Limits, *Neural Computing and Applications*, **1**, (3), pp 224-228, Springer-Verlag London Limited, 1993.
23. DUFFIELD, M.J. Revised fatigue index formula for the dominie T1 wing based on finningley operational 'G' count records, HST.R.252.FG0352, 1985.
24. UK MoD, Ministry of Defence, Joint Service Publication, JSP553, Military Airworthiness Regulations, 1st Ed, 2003.
25. UK MoD Defence Standard 00-970, Design and Airworthiness Requirements for Service Aircraft, Section 3.2.29 – 3.2.55 and Chapter 42 – Structural Monitoring Systems Using Non-Adaptive Prediction Methods, **4**, 2006.


https://doi.org/10.1017/S0001924000002190 Published online by Cambridge University Press